The International Journal of Advanced Manufacturing Technology (2019) 100:2521–2536
https://doi.org/10.1007/s00170-018-2833-9

ORIGINAL ARTICLE

Design of diagonal cross-aisle warehouses with class-based storage assignment strategy

Marco Bortolini[1] · Maurizio Faccio[2] · Emilio Ferrari[1] · Mauro Gamberi[1] · Francesco Pilati[1]

Received: 23 May 2018 / Accepted: 2 October 2018 / Published online: 18 October 2018

Abstract
Non-traditional warehouses shorten the travelled paths to store and retrieve (S/R) the loads, thanks to additional aisles crossing the parallel racks. This paper provides the analytic model to best design a non-traditional warehouse for unit-load (UL) with diagonal cross-aisles and storage policy according to the class-based storage (CBS) strategy. The model minimizes the average single-command cycle time to S/R the loads, best sizing the classes, their shape, and the position/numbers of additional aisles. The focus is on both 2- and 3-CBS optimizing the number of diagonal cross-aisles to best balance the travel time reduction and the loss of storage space due to the aisles. Furthermore, benchmarking toward standard warehouses with no diagonal cross-aisles and random assignment strategy allows quantifying the positive impact of the proposed design configuration on the daily warehouse operations.

Keywords Non-traditional warehouse · Warehouse design · Class-based storage · Diagonal cross-aisle · Warehouse operations

1 Introduction

The scientific community and the industrial practitioners often stress the crucial role of warehouse management to increase the performances of the storage systems working in the modern industrial companies [1–3]. According to Gu et al. [4], such a managerial discipline includes warehouse design and warehouse operation as the two key macro-areas made of strategic, tactical, and operative levels of decision [5]. The former macro-area deals with the effective design of the storage volume, matching predefined technical, cost, and environmental performances [6, 7]; the latter macro-area deals with decisions on the daily warehousing activities to store and retrieve (S/R) the materials [4].

Focusing on the warehouse design, the literature agrees to introduce five interrelated decisions to take, i.e., overall structure, department layout, sizing and dimensioning, equipment selection, and operation strategy (see [4, 8] for a detailed discussion of the goals to achieve). In parallel, a panel of measurement indicators quantifies the system performances along the time, quality, cost, and productivity dimensions [9–11].

Unit-load (UL) warehouses are diffuse solutions to receive, store, and ship items stocked in pallets [12]. Their best design is essential to increase the inbound logistic performances and to reduce the operative handling and inventory costs [13, 14]. Rouwenhorst et al. [5] defined the warehouse design as "a structured approach of decision making to meet a number of well-defined performance criteria" and point out the following three decisional levels:

- Strategic level, facing the long term, e.g., 5 yearlong, decisions;
- Tactical level, facing the medium term, e.g., 2 yearlong, decisions;
- Operational level, facing the short term, e.g., 1 yearlong or below, decisions.

Such decisional levels intersect the following decisional categories to face, as widely discussed by Gu et al. [7]:

✉ Marco Bortolini
marco.bortolini3@unibo.it

[1] Department of Industrial Engineering, Alma Mater Studiorum, University of Bologna, Viale del Risorgimento, 2, 40136 Bologna, Italy

[2] Department of Management and Engineering, University of Padova, Stradella San Nicola, 3, 36100 Vicenza, Italy

- Structure conceptual design, about the number of storage departments, the adopted technologies, and the order fulfillment methods, typical of the strategic level;
- Sizing and dimensioning, to set the storage capacity and floor space, typical of the strategic and tactical levels;
- Warehouse layout, about the shape and the pickup and delivery (P&D) point position, typical of the tactical level;
- Equipment selection, about the best level of automation, the type of storage and material handling systems, typical of the tactical and operative levels;
- Operation policy selection, about the storage/retrieval policies and adopted command cycles, typical of the operative level [4].

The introduced decisional levels and categories are strongly interrelated with fruitful bottom-up feedbacks [15, 16].

This paper faces the warehouse layout decisions at the *tactical level*. Particularly, the goal is to analyze the impact of a non-traditional warehouse configuration on the average single-command cycle time in the case of class-based storage (CBS) assignment strategy.

Traditionally, industrial warehouse racks are arranged to create parallel picking aisles with a front access area and, sometimes, one or more orthogonal aisles to further facilitate the flow among the picking aisles. In the recent past, non-traditional configurations rose up to speed the access to the storage locations. Effective examples are the so-called flying-V and fishbone rack layouts designed by Gue and Meller [12] and the chevron, leaf, and butterfly rack layouts designed by Öztürkoğlu et al. [17]. Such configurations differ for the rack orientation with respect to the P&D point and the warehouse boundaries, but they share the common assumption of including one or more additional aisles, called diagonal cross-aisles in the following, crossing the racks and allowing shorter paths with respect to the rectilinear orthogonal paths of traditional warehouses. In this paper, to join the time savings due to the diagonal cross-aisles and to ease the operative feasibility of such a non-traditional configuration, the rack orientation is not changed and the diagonal cross-aisles are supposed to be straight, i.e., rectilinear. The reference warehouse schematic is in Fig. 1, further highlighting the position of the P&D point, supposed to be at the center of the front of the racks.

In addition, this paper adopts the CBS assignment strategy of the ULs into the racks. According to Le-Duc and de Koster [18], CBS means dividing the items into classes based on their picking frequencies and the storage locations into a same number of zones. Each class is assigned to a zone so that the fastest moving classes are closest to the P&D point. Since Hausman et al. [19], CBS is considered effective to implement, allowing a strong reduction of the travelled distances toward random storage assignment [20, 21]. The zone shapes depend on the warehouse features and the available paths so that the inclusion of diagonal cross-aisles affects them. The proposed model addresses the optimization of the class shapes together with the diagonal cross-aisle best positioning. The optimization of non-traditional UL warehouses with CBS assignment strategy is innovative and recognized as a literature open-topic to address [20–22].

Finally, a predictable weakness of including additional diagonal cross-aisles into a storage system is the loss of storage capacity [17]. The higher the number of diagonal cross-aisles and the lower the size of the warehouse, the higher the incidence of the storage loss on the available space is. A model to estimate the relative storage capacity loss is proposed by Bortolini et al. [22] and used here to trade-off the distance savings and the loss of UL locations.

According to the introduced topic and purposes, the remainder of this paper is organized as in the following. The next section (section 2) revises the literature, while section 3 introduces the model assumptions and benchmark scenarios. Section 4 widely describes the analytic models to compute the average single-command travel distance and to optimize the non-traditional CBS warehouse for both 2- and 3-CBS

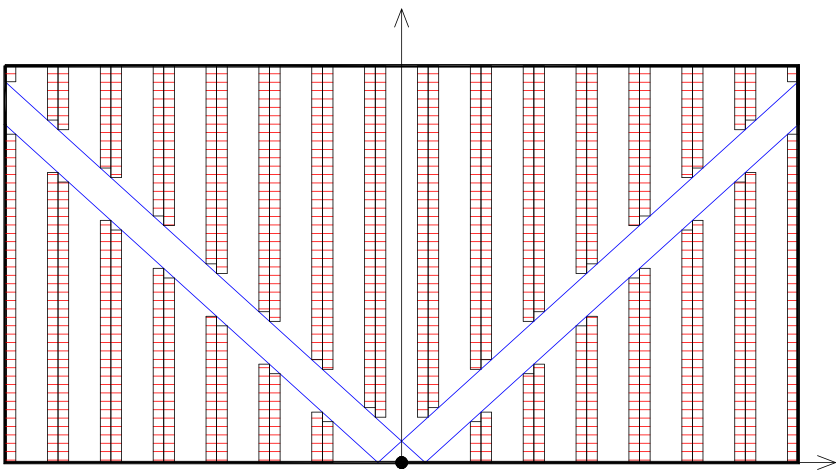

Fig. 1 Non-traditional warehouse configuration with straight diagonal cross-aisles

systems. Section 5 applies the proposed model to an industrial case study before concluding the paper with remarks and future research suggestions in the last section (section 6).

2 Literature review

Warehouse design is a strategic issue affecting the handling and storage performances together with the company cost structure. Rouwenhorst et al. [5] and Gu et al. [7] classified the literature contributions highlighting effective criteria to systematically face the decision making process. Based on their works, Dotoli et al. [11] proposed a scheme for warehouse analysis and optimization based on anomalies identification, rank, and update through technological and managerial changes, while Accorsi et al. [9] included multiple perspectives in the warehouse building design problem dedicating specific attention to the economic [23], environmental [24], and efficiency [25] perspectives. In addition, the recent literature dedicated attention to some industrial sectors having specific peculiarities due to the product storage requirements. Reference examples are within the cold chain for food [26, 27], pharmaceutical [28], and chemical [29, 30] industries.

Focusing on the warehouse aisle design and general layout, Bassan et al. [31] developed models to define the best position of the picking aisles assuming standard racks. White [32] firstly discussed the benefit coming from a non-traditional warehouse design and introduced radial aisles crossing the racks. Arlinghaus and Nystuen [33] focused on the effect of a diagonal link in a rectangular grid network, while Gue and Meller [12] introduced the aforementioned flying-V and fishbone warehouse layouts for UL warehouses with random storage assignment strategy. Clark and Meller [34] and Cardona et al. [35] extended the analysis to include the vertical travel distance, while Çelk and Süral [36] investigated order picking policies to S/R products in a fishbone storage system. Pohl et al. [37, 38] analyzed the impact of dual-command cycles on the warehouse design problem and on the fishbone aisle optimization. Furthermore, Gue et al. [39] and Thomas and Meller [40] considered a non-conventional aisle design with multiple P&D points. Öztürkoglu et al. [17] developed the introduced chevron, leaf, and butterfly rack layouts, while Bortolini et al. [22] presented straight diagonal cross-aisle non-traditional warehouse. Finally, Pferschy and Schauer [41] focused the attention on non-standard warehouse in the emerging e-commerce business. All the authors designed their warehouses assuming a random and continuous storage assignment of the ULs.

Concerning the product assignment, three strategies are adopted in the most of the operative contexts. Randomized strategy (1) assigns products to the first available location, dedicated storage strategy (2) assigns each product to specific locations, while CBS strategy (3) assigns each class of similar products to a predefined zone of the warehouse according to the picking frequencies. Heskett [42], Kallina and Lynn [43], Roodbergen and de Koster [15], Manzini et al. [44], and Gue and Meller [12] widely discussed such strategies defining the most convenient applicability ranges. CBS emerges as an effective strategy to compensate the major weaknesses of the other two [14]. Examples of contributions on both UL and order picking CBS warehouses are in Larson et al. [45], Kovács [46], Ene and Oztürk [47], Rao and Adil [48], Yu and de Koster [49], and Ekren et al. [50]. Furthermore, within CBS strategy, starting from Flores and Whybark [51], multiple criteria are considered to define the classes within multi-criteria inventory classification models. Lolli et al. [52, 53] presented a useful framework based on five steps and tailored for intermitted demand items, while Ishizaka et al. [54] integrated data envelopment analysis (DEA) to analytic hierarchy process (AHP) to sort items into ordered classes. Soylu and Akyol [55] stressed the role of the decision maker preferences in the class definition, while Douissa and Jabeur [56] and Torabi et al. [57] presented multi-criteria methods joining qualitative and quantitative classification drivers. Having the products ranked in order of preference is the base step to assign them to the warehouse classes and, then, to the available storage locations. In this field, as far as the authors' knowledge, all the contributions considered traditional warehouses with parallel picking aisles and no diagonal cross-aisles as the reference storage system for the product assignment.

The analysis of the past and recent literature highlights that studies on the design of non-traditional warehouses with CBS assignment strategy are still missing. Starting from this background and the literature open issues, the present contribution addresses the design of non-traditional CBS systems including one or multiple straight diagonal cross-aisles. The analytic models for the best positioning of such aisles and the optimal class sizing and shaping are proposed quantifying the correspondent distance savings with respect to the traditional warehouse configuration, further including the storage capacity loss due to the presence of the additional diagonal cross-aisles.

3 Model assumptions and benchmark scenario

The proposed model computes the mean travel distance between the P&D point and a generic point into the UL-CBS system. Two design drivers identify each of the considered scenarios:

- the number of additional diagonal cross-aisles; and
- the number of classes in the CBS system.

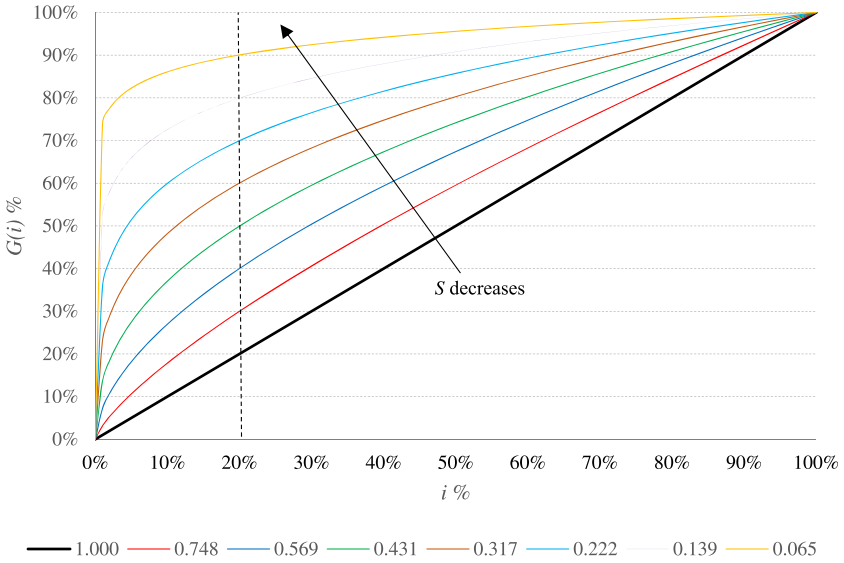

Fig. 2 Normalized cumulative demand waveforms varying the skewness factor

In the following, D_{ac} identifies the average travelled distance model with a diagonal cross-aisles and c classes. As example, D_{01}, D_{02}, and D_{03} refer to the zero diagonal cross-aisles, random, and 2- and 3-CBS systems, i.e., the reference benchmark, while D_{1c} and D_{2c} are for single and double diagonal cross-aisle systems with c classes. For each scenario, the class shapes and diagonal cross-aisle positions (if present) are calculated, minimizing the average travelled distance to S/R the ULs. All the considered scenarios share the following set of assumptions:

1. the warehouse is for ULs with single-command cycles;
2. the P&D point is located in the lower center of the aisles, origin of axis;
3. the warehouse is symmetric respect to the y-axis. Without loss of generality, the right side is focused in the model;
4. the warehouse shape ratio is 2:1 and normalized dimensionless racks are used;
5. all the products have the same dimensions and they are continuously distributed into the racks;
6. the S/R locations are independent and identically distributed (i.i.d.), and the access to the available locations follows the CBS assignment strategy;
7. the ULs are split into the classes according to their demand level. Inside each class, the UL assignment is random. The well-known demand curve $G(i) = i^S$ is adopted [19], where:

- i is the normalized cumulative storage area for all products, ranking them in decreasing order of the ratio between the demand and the storage area, [0,1];
- S is the so-called skewness factor, (0,1];
- $G(i)$ is the normalized cumulative demand until the ith percentile of the storage area. It represents the probability of access to a generic UL within the storage area i, [0,1].

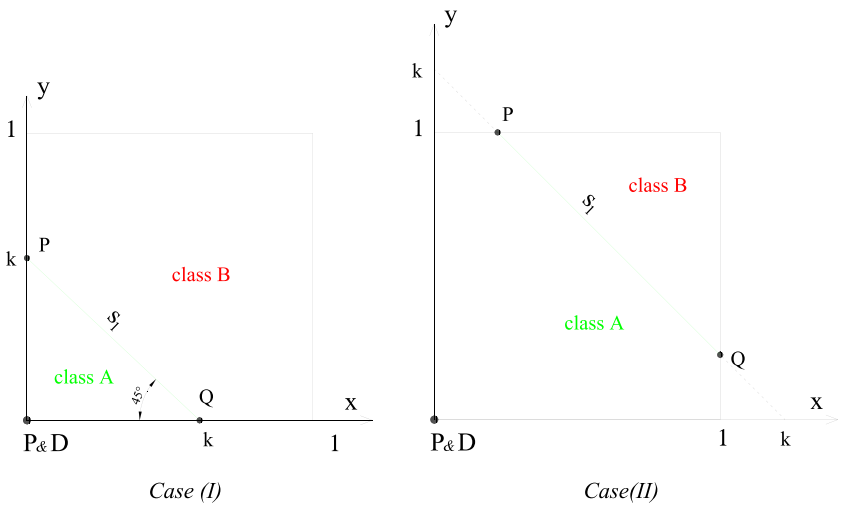

Fig. 3 D_{02} storage system configurations

Table 1 Results for the D_{02} benchmark scenario. For cumulative ABC curves, in the notation XX%–YY%, XX identifies the percentage of stored loads, while YY identifies the cumulative demand frequency, e.g., 20–80% curve means that the 20% of the stored loads involves the 80% of the total demand of the S/R operations

ABC curve	S	k^{opt}	D_{02}^{opt}
Random	1.000	–	1.000
20–30%	0.748	0.730	0.926
20–40%	0.569	0.652	0.855
20–50%	0.431	0.574	0.782
20–60%	0.317	0.491	0.701
20–70%	0.222	0.400	0.608
20–80%	0.139	0.295	0.493
20–90%	0.065	0.165	0.330

Figure 2 presents typical waveform profiles of the demand curve varying the skewness factor.

As discussed in section 2, alternative criteria to the demand level to create classes exist, e.g., multi-criteria inventory classification models [51–57], leading to different curves with respect to those of Fig. 2 and ranking the products in other orders of preference. Nevertheless, because such curves are among the input, the model presented in the following remains valid even in the case of alternative product classification models.

The following paragraph discusses the model for the benchmark scenario, i.e., no diagonal cross-aisles.

3.1 Benchmark scenarios with no diagonal cross-aisles

In the benchmark scenario, the distance to connect the P&D point to a generic location $P(x, y)$ is $f(x, y) = x + y$ according to the existing orthogonal paths. In the case of UL random assignment to the bays, the average travelled distance is, trivially, $D_{01} = 1$ because the average bay coordinates, in the normalized space, are (0.5, 0.5).

Adopting the CBS strategy, Fig. 3 depicts the configurations for the D_{02} scenario, further introducing the key notations. The class shapes are univocally defined by the storage area boundaries and the line s_1. Such a line is called *equi-*

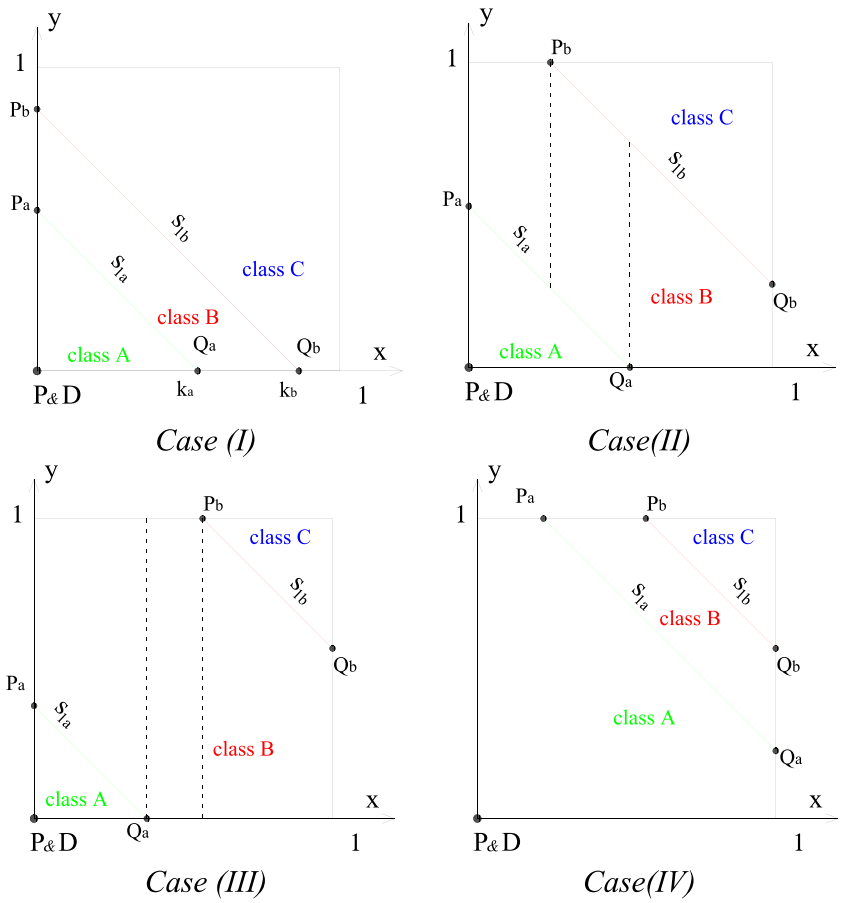

Fig. 4 D_{03} storage system configurations

Table 2 Results for the D_{03} scenario

ABC curve	S	k_A^{opt}	k_B^{opt}	D_{03}^{opt}
Random	1.000	–	–	1.000
20–30%	0.748	0.478	0.974	0.909
20–40%	0.569	0.397	0.905	0.821
20–50%	0.431	0.323	0.835	0.731
20–60%	0.317	0.252	0.762	0.633
20–70%	0.222	0.183	0.682	0.525
20–80%	0.139	0.116	0.588	0.398
20–90%	0.065	0.052	0.467	0.236

distance line in the following and represents the locus of points whose distance from the P&D point is equal to a defined constant value, k. Its equation is $s_1 : x + y = k$. The value of k, univocally defining the class shape, also determines the class size and it is among the variables to optimize according to the skewness factor, S, of the considered case.

Figure 3 shows two cases depending on the position of s_1 with respect to the bisector line, i.e., case (I) is for $0 \le k \le 1$ and case (II) is for $1 < k \le 2$. For each case, the average distances from the P&D point to a generic point inside the class A, D_{02}^A, and B, D_{02}^B, are computed through the Integral Mean Value Theorem. Integrals are extended to the class areas, A_A and A_B. Equations (1)–(2) shows the expressions to get D_{02}^A and D_{02}^B for case (I), while Eqs. (3)–(4) are for case (II). For the sake of brevity, the closed forms coming from the integral solution are omitted. Furthermore, in Eqs. (1)–(4), the notations Q^x and P^x symbolize the x coordinate of points Q and P of Fig. 3.

$$D_{02}^A = \frac{1}{A_A}\int_0^{Q^x}\int_0^{s_1} f(x,y)dydx \tag{1}$$

$$D_{02}^B = \frac{1}{A_B}\left(\int_0^{Q^x}\int_{s_1}^{1} f(x,y)dydx + \int_{Q^x}^{1}\int_0^{1} f(x,y)dydx\right) \tag{2}$$

$$D_{02}^A = \frac{1}{A_A}\left(\int_0^{P^x}\int_0^{1} f(x,y)dydx + \int_{P^x}^{1}\int_0^{s_1} f(x,y)dydx\right) \tag{3}$$

$$D_{02}^B = \frac{1}{A_B}\int_{P^x}^{1}\int_{s_1}^{1} f(x,y)dydx \tag{4}$$

The overall average distance, D_{02}, is calculated weighting the values obtained for the two classes by the class access probabilities coming from the introduced demand curve (see assumption 7) as in Eq. (5).

$$D_{02} = D_{02}^A \cdot G(A_A) + D_{02}^B \cdot (1 - G(A_A)) \tag{5}$$

Table 1 shows the optimal values of k, minimizing D_{02}, for typical values of the demand curve, including the random scenario ($S = 1$). To minimize D_{02}, the Sequential Quadratic Programming (SQP) numerical optimization algorithm is applied through a dedicated Maple® interface [58].

Results highlight that k^{opt} and D_{02}^{opt} decrease if S decreases: low values of the skewness factor mean that a high percentage of the demand is generated by a small percentage of the loads so that both the class A area and the average travelled distance

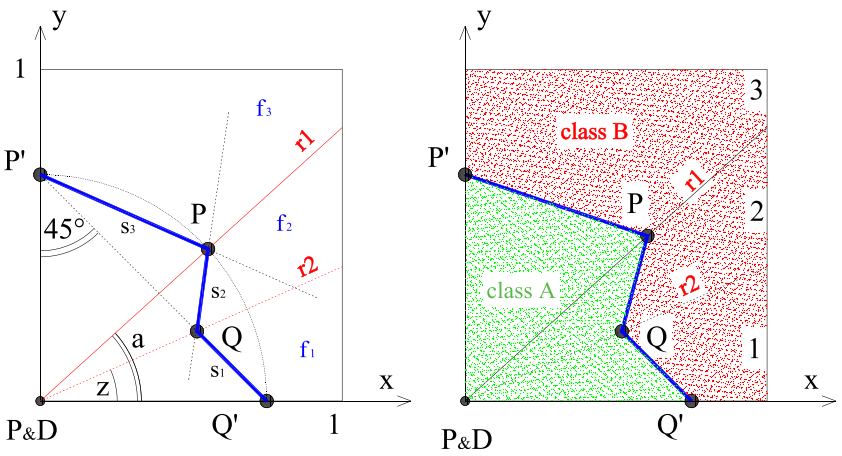

Fig. 5 Reference layout and notations for D_{12} scenario

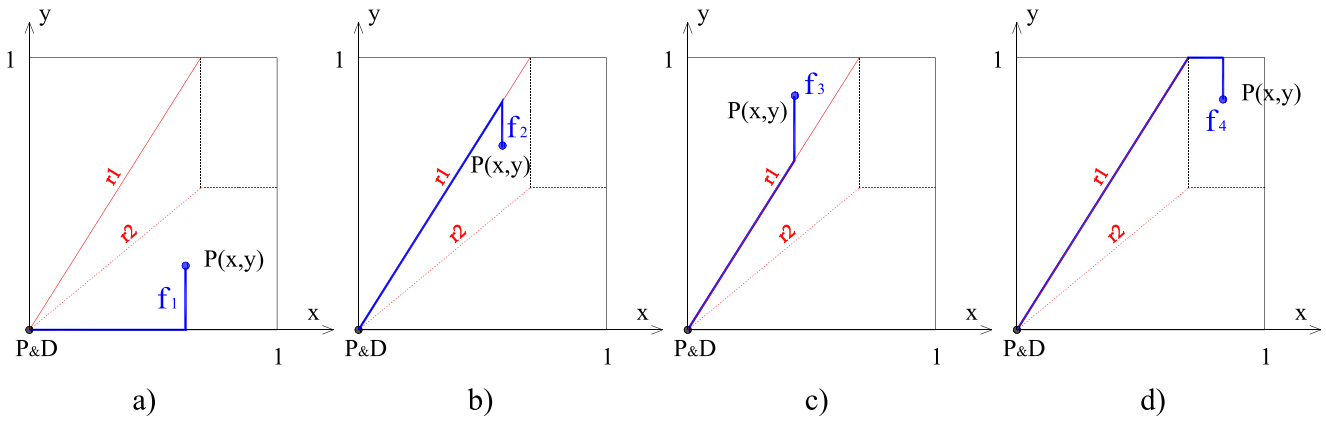

Fig. 6 Access zones in the normalized storage area with one diagonal cross-aisle

are small. Finally, the optimal position of s_1 falls in case (I) ($0 \le k \le 1$) for all the values of the skewness factor.

Adding the third class means referring to the four cases and notations of Fig. 4, where $s_{1A} : y = -x + k_A$ and $s_{1B} : y = -x + k_B$ define the boundaries of the classes.

The equations to compute the average travelled distance for the four cases and the three classes, namely A, B, and C, are detailed in Eqs. (24)–(36) at the end of the paper, while in the case of the 3-CBS system, Eq. (5) becomes the following to get D_{03}.

$$D_{03} = D_{03}^{A} \cdot G(A_A) + D_{03}^{B} \cdot (G(A_A + A_B) - G(A_A)) + D_{03}^{C} \cdot (1 - G(A_A + A_B)) \quad (6)$$

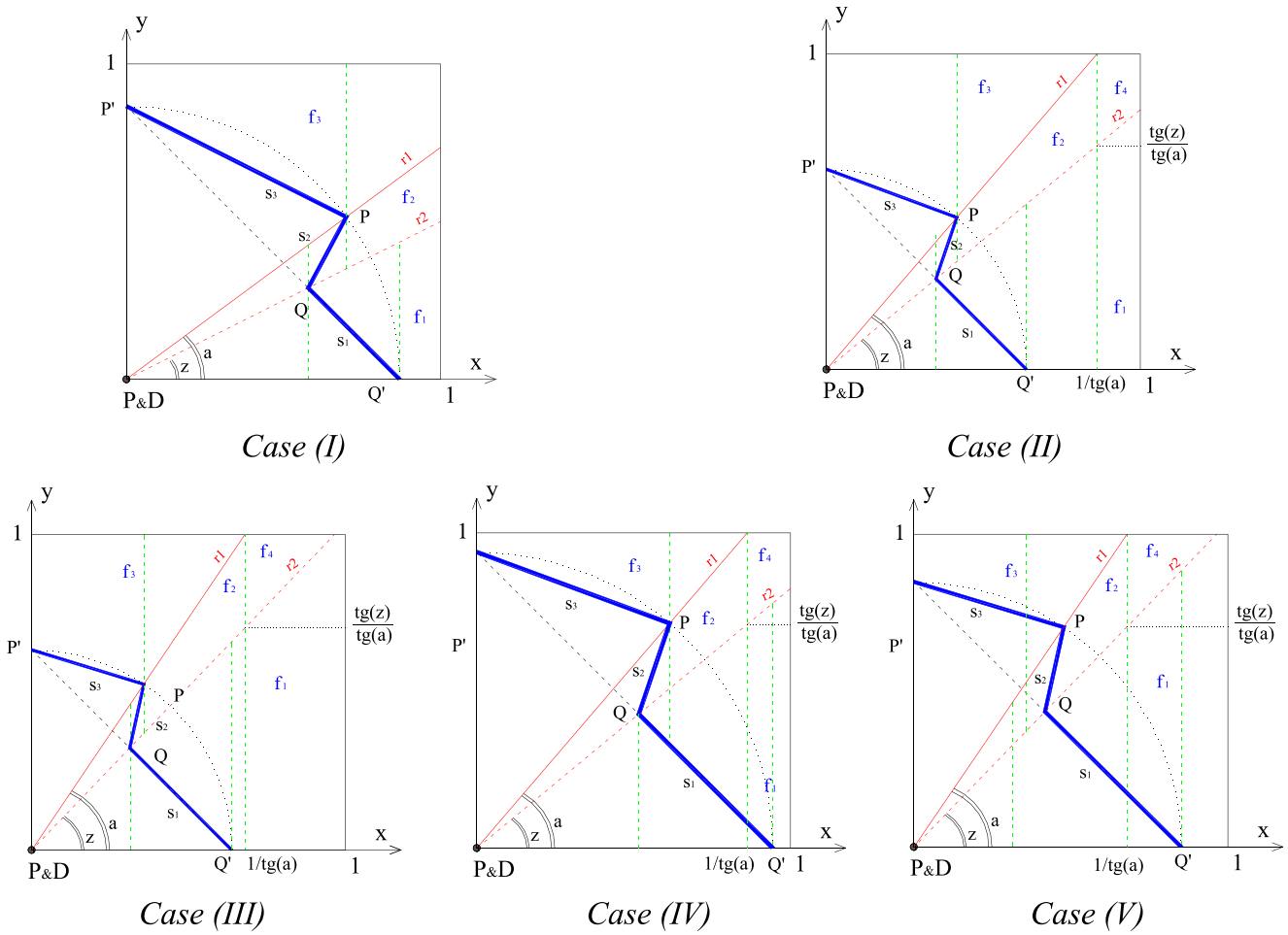

Fig. 7 D_{12} storage system configurations

Table 3 Results for the D_{12} scenario

ABC curve	S	k^{opt}	a^{opt}	D_{12}^{opt}
Random	1.000	–	33.97°	0.853
20–30%	0.748	0.626	33.93°	0.792
20–40%	0.569	0.560	33.90°	0.733
20–50%	0.431	0.493	33.88°	0.672
20–60%	0.317	0.421	33.86°	0.603
20–70%	0.222	0.343	33.84°	0.524
20–80%	0.139	0.253	33.83°	0.425
20–90%	0.065	0.141	33.83°	0.284

Table 2 presents the optimal values for the D_{03} scenario.

As for D_{02}, the average travelled distance is lower for low values of the skewness factor and case (I) ($0 \le k_A \le k_B \le 1$) always includes the optimal warehouse configuration. Finally, given the demand curve, the inclusion of the third class reduces the travelled distance between 1.90 and 28.46% with respect to the equivalent two-class configurations. The lower the values of S, the higher the savings are.

Starting from these benchmarks, section 4 describes the analytic models to compute the average single-command travel distance optimizing the non-traditional CBS warehouse with diagonal cross-aisles. In the following, for brevity, for each scenario, the case containing the optimum is presented only.

4 Diagonal cross-aisle warehouse with CBS assignment strategy

This section discusses the models for one and two diagonal cross-aisles with two and three classes. The description of the random storage assignment scenarios with one and two diagonal cross-aisles, i.e., D_{11} and D_{21}, is detailed by Bortolini et al. [22]. The full description of the D_{12} scenario is proposed, while the key results for the other scenarios are listed.

4.1 One diagonal cross-aisle 2-CBS distance model—D_{12}

Figure 5 depicts the configuration and the key notations for a warehouse with one diagonal cross-aisle and two classes.

The position of the diagonal cross-aisle, r_1, is univocally defined by the angle a. r_1 equation is $y = \tan(a) \cdot x$. The red dashed line, r_2, is called the *iso-distance line* in the following, and it is the locus of points whose distances from the P&D point choosing the bottom front aisle and up the picking aisle or moving along the diagonal cross-aisle and down the picking aisle are the same [22]. The position of r_2 is fixed by the angle $z(a)$, function of a, and the r_2 equation is $y = \tan(z(a)) \cdot x$. The piecewise-defined blue line is the new *equi-distance line* introduced in the previous section. Its shape is different, like a "bolt", due to the presence of r_1 and r_2 (for its analytical definition, the reader can refer to the lines s_1, s_2,and s_3 presented below).

r_1 and r_2 split the storage area into four zones, as shown in Fig. 6. A generic location $P(x, y)$ inside zone 1 is accessible by moving horizontally and then vertically inside the picking aisle (distance function f_1 of Fig. 6a), while locations in zone 2 are accessible through the diagonal cross-aisle and then moving down vertically (distance function f_2 of Fig. 6b). Locations in zone 3 are accessible through the diagonal cross-aisle and then moving up vertically (distance function f_3 of Fig. 6c). Finally, locations in zone 4 are accessible by travelling along the diagonal cross-aisle, moving

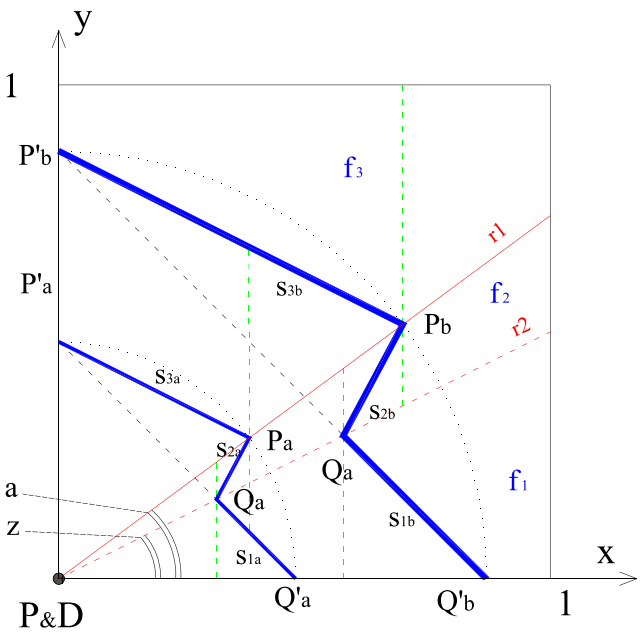

Fig. 8 D_{13} storage system best configuration

Table 4 Results for the D_{13} scenario

ABC curve	S	k_A^{opt}	k_B^{opt}	a^{opt}	D_{13}^{opt}
Random	1.000	–	–	33.97°	0.853
20–30%	0.748	0.405	0.826	33.92°	0.778
20–40%	0.569	0.338	0.770	33.88°	0.705
20–50%	0.431	0.275	0.712	33.84°	0.629
20–60%	0.317	0.215	0.651	33.81°	0.546
20–70%	0.222	0.157	0.584	33.79°	0.454
20–80%	0.139	0.100	0.504	33.77°	0.344
20–90%	0.065	0.044	0.399	33.76°	0.204

horizontally on top of the storage area (through an upper side aisle) and then moving down inside the picking aisle (distance function f_4 of Fig. 6d). Zone 4 is not present if the diagonal cross-aisle intersects the vertical side of the storage area, i.e., $\tan(a) \leq 1$.

For each zone, i, the analytic expressions of the distance function, $f_i(x, y)$, between the P&D point and a generic $P(x, y)$ location inside the ith zone are in the following.

$$f_1(x,y) = x + y \tag{7}$$

$$f_2(x,y) = \frac{x}{\cos(a)} - y + x \cdot \tan(a) \tag{8}$$

$$f_3(x,y) = \frac{x}{\cos(a)} + y - x \cdot \tan(a) \tag{9}$$

$$f_4(x,y) = \frac{1}{\sin(a)} + x - \frac{1}{\tan(a)} + 1 - y \tag{10}$$

Furthermore, the analytic expression of $z(a)$ is by equating Eqs. (8) and (9). Its analytic expression is:

$$z(a) = \tan^{-1}\left(\frac{1 + \sin(a) - \cos(a)}{2 \cdot \cos(a)}\right) \tag{11}$$

Due to the different paths to enter the picking aisles, the shape of the classes is different with respect to the reference scenarios. Figure 7 presents the cases for the D_{12} scenario. Differences among the cases are due to the relative position of points P, P', Q, and Q' compared to the intersection point of r_1 with the warehouse top side (see the dashed green lines in Fig. 7). This circumstance affects the integration domains of the functions f_1, f_2, f_3, and f_4 for the evaluation of the mean travel distance within each zone (refer to Eqs. (37)–(46) at the end of the paper for the integral details).

The shape of the *equi-distance* line is different into each zone of Fig. 7 and it is defined by the segments QQ', PQ, and $P'P$ on s_1, s_2, and s_3. The points P', Q', and P lie on the circle of center $P\&D$ and radius k (the same distance from $P\&D$). They are determined by its intersection with the y-axis, x-axis, and the diagonal cross-aisle r_1, respectively. Definitively $P'(0, k)$, $Q'(k, 0)$ and $P(k \cdot \cos(a), k \cdot \sin(a))$. Finally, Q is the point of intersection between r_2 and s_1. Its coordinates are

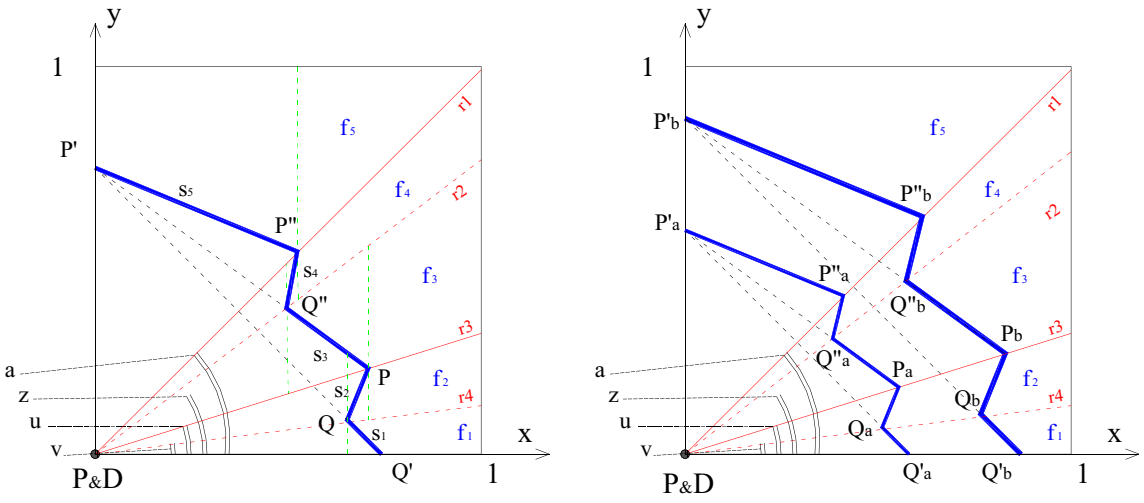

Fig. 9 D_{22} and D_{23} storage system best configurations

Table 5 Results for the D_{22} scenario

ABC curve	S	k^{opt}	u^{opt}	a^{opt}	D_{22}^{opt}
Random	1.000	–	22.95°	42.60°	0.822
20–30%	0.748	0.604	22.83°	42.66°	0.764
20–40%	0.569	0.540	22.74°	42.71°	0.707
20–50%	0.431	0.475	22.67°	42.75°	0.648
20–60%	0.317	0.406	22.62°	42.79°	0.581
20–70%	0.222	0.331	22.58°	42.82°	0.505
20–80%	0.139	0.244	22.55°	42.84°	0.410
20–90%	0.065	0.136	22.55°	42.84°	0.274

$\left(\frac{k}{\tan(z(a))+1}, \frac{k}{\tan(z(a))+1}\right)$. Given P', P, Q', and Q, the lines s_1, s_2, and s_3 follow. Equations (12)–(13) detail s_2 and s_3, while s_1 is already defined in section 3.1.

$$s_2 : y = \left(\frac{1}{\cos(a)} + \tan(a)\right) \cdot x - k \tag{12}$$

$$s_3 : y = -\left(\frac{1}{\cos(a)} + \tan(a)\right) \cdot x + k \tag{13}$$

As for the benchmark scenario, D_{12}^A and D_{12}^B are evaluated through the Integral Mean Value Theorem extending the integrals to the class areas, A_A and A_B (see Eqs. (37)–(46) at the end of the paper for mathematics). Then, using Eq. (5), D_{12} follows and it is minimized for the same values of the skewness factor presented before. Results are in Table 3.

The optimal size of the class boundary follows the same trend discussed for the benchmark scenario, while the position of the diagonal cross-aisle is very little influenced by the demand curve and it is equal to ~34° in all cases.

4.2 One diagonal cross-aisle 3-CBS distance model—D_{13}

The inclusion of the third class duplicates the class boundaries as described passing from D_{02} to D_{03}. Figure 8 exemplifies this scenario in the case with $a \leq 45^{\circ}$ and $0 \leq k_A \leq k_B \leq 1$. All the other scenarios are tested but results prove that the optimum configuration falls in this case.

The equations to calculate D_{13}^A, D_{13}^B, and D_{13}^C are in Eqs. (47)–(49) at the end of the paper, while the previous Eq. (6) allows getting D_{13}. Table 4 presents the results of the optimization for this scenario.

Similarly to the previous cases, the class dimension decreases if the skewness increases, while the diagonal cross-aisle position is almost constant and it does not change with respect to the D_{12} scenario. In all cases, the angle a is close to 34°.

4.3 Inclusion of the second diagonal cross-aisle: D_{22} and D_{23} models

The inclusion of the second diagonal cross-aisle enlarges the available paths connecting the P&D point to the storage bays, beyond those of Fig. 6, shortening the mean travelled distance with a further reduction of the available storage space. As detailed while introducing the first diagonal cross-aisle, the normalized storage area is partitioned into zones associated to univocal shortest access paths. The following Fig. 9 presents the reference best configurations of the storage system with 2- and 3-CBS system.

The two diagonal cross-aisles are $r_1 : y = \tan(a) \cdot x$ and $r_3 : y = \tan(u) \cdot x$, while the correspondent *iso-distance* lines are $r_2 : y = \tan(z(a)) \cdot x$ and $r_4 : y = \tan(v(u)) \cdot x$ calculated adapting Eq. (11). Furthermore, the upgrades to the $f_i(x, y)$ distance function for the five regions of Fig. 9 are in the following equations.

Table 6 Results for the D_{23} scenario

ABC curve	S	k_A^{opt}	k_B^{opt}	u^{opt}	a^{opt}	D_{13}^{opt}
Random	1.000	–	–	22.95°	42.61°	0.822
20–30%	0.748	0.390	0.796	22.79°	42.69°	0.750
20–40%	0.569	0.325	0.742	22.67°	42.76°	0.680
20–50%	0.431	0.265	0.687	22.58°	42.82°	0.607
20–60%	0.317	0.207	0.628	22.51°	42.87°	0.527
20–70%	0.222	0.151	0.563	22.45°	42.91°	0.438
20–80%	0.139	0.096	0.486	22.40°	42.96°	0.332
20–90%	0.065	0.042	0.385	22.37°	42.99°	0.197

Fig. 10 Result comparison

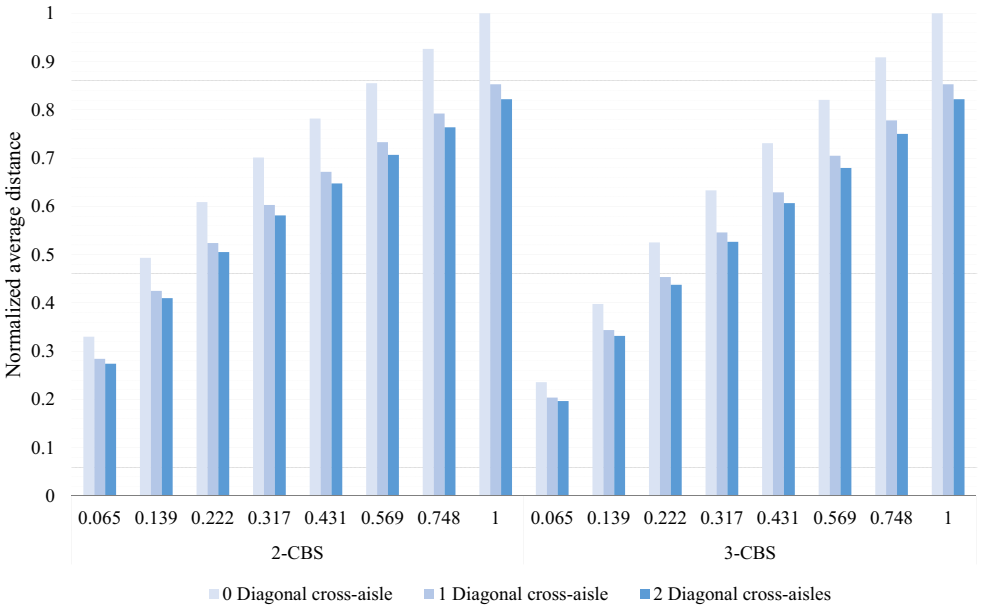

$$f_1(x,y) = x + y \tag{14}$$

$$f_2(x,y) = \frac{x}{\cos(u)} - y + x \cdot \tan(u) \tag{15}$$

$$f_3(x,y) = \frac{x}{\cos(u)} + y - x \cdot \tan(u) \tag{16}$$

$$f_4(x,y) = \frac{x}{\cos(a)} - y + x \cdot \tan(a) \tag{17}$$

$$f_5(x,y) = \frac{x}{\cos(a)} + y - x \cdot \tan(a) \tag{18}$$

$$s_1 : y = -x + k \tag{19}$$

$$s_2 : y = \left(\frac{1}{\cos(u)} + \tan(u)\right) \cdot x - k \tag{20}$$

$$s_3 : y = -\left(\frac{1}{\cos(u)} + \tan(u)\right) \cdot x + k \tag{21}$$

$$s_4 : y = \left(\frac{1}{\cos(a)} + \tan(a)\right) \cdot x - k \tag{22}$$

$$s_5 : y = -\left(\frac{1}{\cos(a)} + \tan(a)\right) \cdot x + k \tag{23}$$

Finally, the *equi-distance* lines limiting the classes are in Eqs. (19)–(23).

In the following, subscripts *A* and *B* allows specifying if the *equi-distance* line is between classes A and B or between

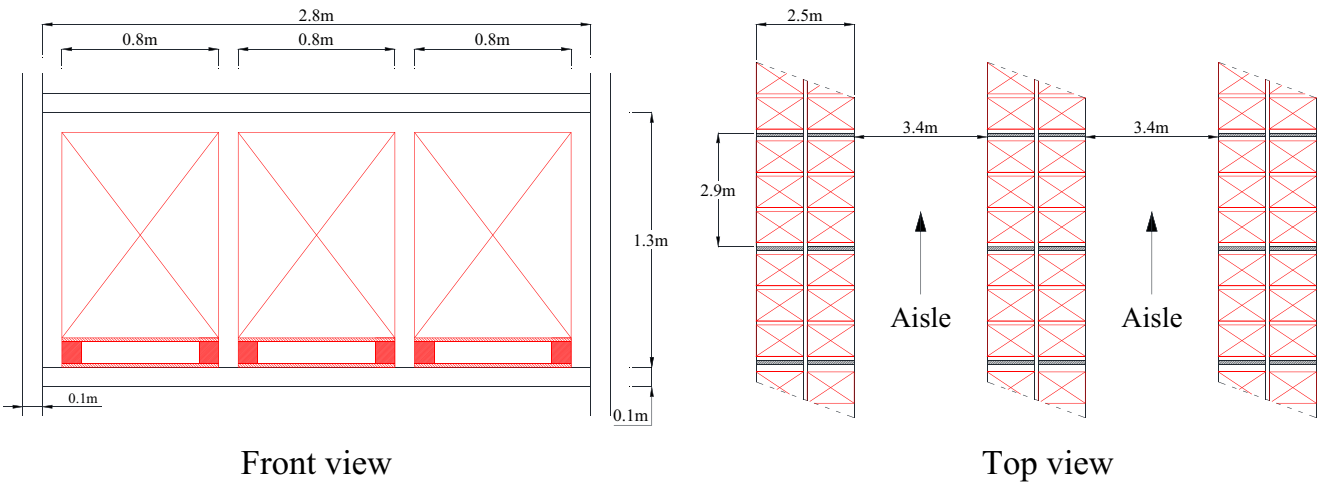

Fig. 11 Rack geometry and aisle and span dimensions

Table 7 Industrial case study results

No. diagonal cross-aisles	D_{a3}^{opt}	u^{opt}	a^{opt}	k_A^{opt}		k_B^{opt}		Saving vs. as-is (%)	Loss of storage capacity (ULs)
				Dimensionless	Real	Dimensionless	Real		
$a=0$	0.525	–	–	0.183	36.7 m	0.682	136.8 m	–	–
$a=1$	0.453	–	33.79°	0.157	31.5 m	0.584	117.2 m	13.71	2059
$a=2$	0.437	22.51°	42.87°	0.151	30.3 m	0.563	112.9 m	16.76	4301

classes B and C. Eqs. (50)–(54) at the end of the paper present the equations to obtain the average travelled distance for each class, in both scenarios. Equations (5) and (6) combine the results getting the final expressions of D_{22} and D_{23}. Minimizing D_{22} and D_{23}, the optimal values in Tables 5 and 6 follow.

The main finding from the system optimization is about the positions of the two diagonal cross-aisles that are almost constant varying the demand skewness factor, i.e., ~23° and ~43° with respect to the front of the storage area. This general conclusion is of strong practical importance because of the warehouse layout and rack positioning is made *ex-ante*, i.e., before assigning products to bays and setting the storage assignment strategy. Having no dependency of the diagonal cross-aisle position on the demand curve and load assignment means that it is not necessary to make continuous re-layouts when the UL assignment changes.

4.4 Result comparison and findings

The results listed in Tables 1, 2, 3, 4, 5, and 6 allow quantifying the impact of the CBS assignment strategy with respect to the random UL assignment varying the demand curve skewness (1) and the number of diagonal cross-aisles (2). Figure 10 collects and compares these results.

As expected, the lower the skewness factor, the lower the average distance is, while the 3-CBS assignment strategy leads to better results than the correspondent 2-CBS scenarios (saving range of 0.5% ÷ 10%). Concerning the diagonal cross-aisle number, the higher they are, the lower the average distance is. Nevertheless, passing from zero to one diagonal cross-aisle generates savings from 4 to 14%, while the inclusion of the second diagonal cross-aisle reduces the average distance below 4% respect to the one diagonal cross-aisle scenarios. Bortolini et al. [22] demonstrated such a decreasing effect for the random assignment strategy that is confirmed here for the CBS assignment strategy.

The major weakness coming from the inclusion of additional diagonal cross-aisles is the storage space loss. Bortolini et al. [22] provide a quantitative method to measure such a loss of space and to correct the average distance to make results refereed to the same net available storage space. Such a methodology is *case-dependent* meaning that the results depend on the size of the storage area and the aisle dimensions. Section 5 presents an application of the proposed design strategy including the analysis of the loss of space.

5 Industrial case study

The proposed approach is applied to redesign the UL, 3-CBS storage system of an Italian company operating in third-part

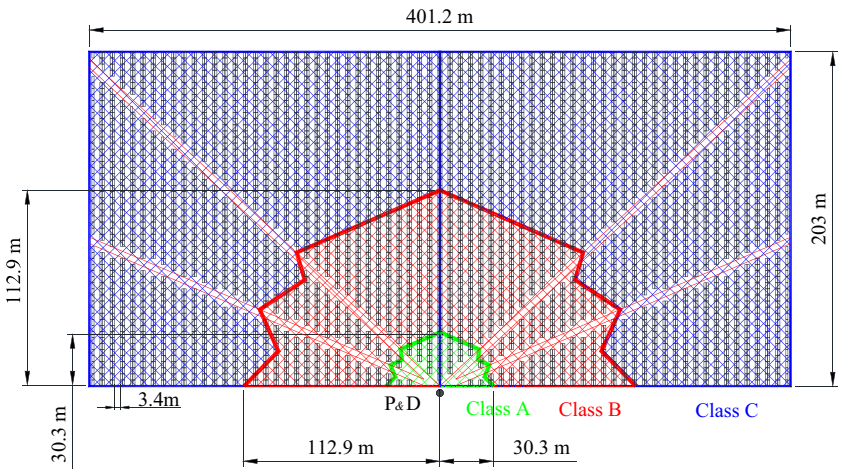

Fig. 12 3-CBS system, 2 diagonal cross-aisle warehouse redesign, case study

transport and logistic services (major information are omitted for privacy).

The ABC analysis on past data allows getting the demand curve. The skewness factor is $S = 0.225$. Furthermore, Fig. 11 shows the rack geometry and the aisle and span dimensions.

The existing storage area is of 401.2×203.0 m with 68 aisles (34 for each half of the warehouse) and 70 spans per aisle. Actually, no diagonal cross-aisle is present so that 28,560 ULs per level can be stored. The following Table 7 compares D_{03}, D_{13}, and D_{23} scenarios given this system configuration calculating, further, the loss of space, expressed in lost storable ULs, as discussed in Bortolini et al. [22].

Because of the company average UL storage requirement at the low level is up to 21,800 ULs, the 3-CBS system with two diagonal cross-aisles scenario, D_{23}, is chosen, saving the 16.76% of the distance at each S/R cycle and increasing the warehouse saturation from 76.3 to 89.9%. Figure 12 presents the effect of the redesign action generating a relevant increase of the handling performances with acceptable loss of space compared to the current company storage requirement.

6 Conclusions and future research directions

This paper aims at supporting the design of non-traditional warehouses for unit-loads (ULs) stored according to the class-based storage (CBS) assignment strategy and retrieved with single-command cycles. The considered system layout includes additional aisles crossing the parallel racks, called diagonal cross-aisles, to reduce the travelled paths. Starting from the literature analysis, stating a gap in providing optimal design models for non-traditional warehouses with CBS strategy, the paper provides the assumptions and the analytic formulations to quantify the average-normalized horizontal distance to perform single-command cycles for 2- and 3-CBS system with zero, one, and two diagonal cross-aisles. For all scenarios, the percentage savings toward the traditional configuration are calculated varying the demand curve shape. In addition, an industrial case study applies the proposed design strategy further quantifying the storage capacity losses due to the introduced diagonal cross-aisles. Results state that the best position of the additional aisles is very low dependent on the demand curve, decoupling the warehouse rack design to the UL assignment. Savings to store and retrieve (S/R) ULs are up to 17% in the industrial test case. Globally, if the demand curve is more skewed, the distance saving increases.

Future research is in twofold directions. On one side, model extensions are possible including dual-command cycles, vertical distances, and rectangular storage areas, i.e., shape factor lower than one. On the other side, the design strategy application to multiple relevant contexts is expected to spread non-traditional warehouses into industry.

Integrals to get D_{03} terms

Case (I)

$$D_{03}^{A} = \frac{1}{A_A}\int_0^{Q_A^x}\int_0^{s_{1A}} f(x,y)dydx \tag{24}$$

$$D_{03}^{B} = \frac{1}{A_B}\left(\int_0^{Q_A^x}\int_{s_{1A}}^{s_{1B}} f(x,y)dydx + \int_{Q_A^x}^{Q_B^x}\int_0^{s_{1B}} f(x,y)dydx\right) \tag{25}$$

$$D_{03}^{C} = \frac{1}{A_C}\left(\int_0^{Q_B^x}\int_{s_{1B}}^{1} f(x,y)dydx + \int_{Q_B^x}^{1}\int_0^{1} f(x,y)dydx\right) \tag{26}$$

Case (II)

$$D_{03}^{A} = \frac{1}{A_A}\int_0^{Q_A^x}\int_0^{s_{1A}} f(x,y)dydx \tag{27}$$

$$D_{03}^{B} = \frac{1}{A_B}\left(\int_0^{P_B^x}\int_{s_{1A}}^{1} f(x,y)dydx + \int_{P_B^x}^{Q_A^x}\int_{s_{1A}}^{s_{1B}} f(x,y)dydx + \int_{Q_A^x}^{1}\int_0^{s_{1B}} f(x,y)dydx\right) \tag{28}$$

$$D_{03}^{C} = \frac{1}{A_C}\int_{P_B^x}^{1}\int_{s_{1B}}^{1} f(x,y)dydx \tag{30}$$

Case (III)

$$D_{03}^{A} = \frac{1}{A_A}\int_0^{Q_A^x}\int_0^{s_{1A}} f(x,y)dydx \tag{31}$$

$$D_{03}^{B} = \frac{1}{A_B}\left(\int_0^{Q_A^x}\int_{s_{1A}}^{1} f(x,y)dydx + \int_{Q_A^x}^{P_B^x}\int_0^{1} f(x,y)dydx + \int_{P_B^x}^{1}\int_0^{s_{1B}} f(x,y)dydx\right) \tag{32}$$

$$D_{03}^{C} = \frac{1}{A_C}\int_{P_B^x}^{1}\int_{s_{1B}}^{1} f(x,y)dydx \tag{33}$$

Case (IV)

$$D_{03}^{A} = \frac{1}{A_A}\left(\int_0^{P_A^x}\int_0^{1} f(x,y)dydx + \int_{P_A^x}^{1}\int_0^{s_{1A}} f(x,y)dydx\right) \tag{34}$$

$$D_{03}^{B} = \frac{1}{A_B}\left(\int_{P_A^x}^{P_B^x}\int_{s_{1A}}^{1} f(x,y)dydx + \int_{P_B^x}^{1}\int_{s_{1A}}^{s_{1B}} f(x,y)dydx\right) \tag{35}$$

$$D_{03}^{C} = \frac{1}{A_C}\int_{P_B^x}^{1}\int_{s_{1B}}^{1} f(x,y)dydx \tag{36}$$

Integrals to get D_{12} terms

Case (I)

$$D_{12}^{A} = \frac{1}{A_A}\left(\int_0^{Q^x}\int_0^{r_2} f_1(x,y)dydx + \int_{Q^x}^{Q'^x}\int_0^{s_1} f_1(x,y)dydx + \int_0^{Q^x}\int_{r_2}^{r_1} f_2(x,y)dydx + \int_{Q^x}^{P^x}\int_{s_2}^{r_1} f_2(x,y)dydx + \int_0^{P^x}\int_{r_1}^{s_3} f_3(x,y)dydx\right) \tag{37}$$

$$D_{12}^{B}=\frac{1}{A_B}\left(\int_{Q^x}^{Q'^x}\int_{s_1}^{r_2}f_1(x,y)dydx+\int_{Q'^x}^{1}\int_{0}^{r_2}f_1(x,y)dydx+\int_{Q^x}^{P^x}\int_{r_2}^{s_2}f_2(x,y)dydx+\int_{P^x}^{1}\int_{r_2}^{r_1}f_2(x,y)dydx+\int_{0}^{P^x}\int_{s_3}^{1}f_3(x,y)dydx+\int_{P^x}^{1}\int_{r_1}^{1}f_3(x,y)dydx\right) \tag{38}$$

Case (II) and Case (III)

$$D_{12}^{A}=\frac{1}{A_A}\left(\int_{0}^{Q^x}\int_{0}^{r_2}f_1(x,y)dydx+\int_{Q^x}^{Q'^x}\int_{0}^{s_1}f_1(x,y)dydx+\int_{0}^{Q^x}\int_{r_2}^{r_1}f_2(x,y)dydx+\int_{Q^x}^{P^x}\int_{s_2}^{r_1}f_2(x,y)dydx+\int_{0}^{P^x}\int_{r_1}^{s_3}f_3(x,y)dydx\right) \tag{39}$$

$$\begin{aligned}D_{12}^{B}=\frac{1}{A_B}\Bigg(&\int_{Q^x}^{Q'^x}\int_{s_1}^{r_2}f_1(x,y)dydx+\int_{Q'^x}^{\frac{1}{\tan(a)}}\int_{0}^{r_2}f_1(x,y)dydx\\&+\int_{\frac{1}{\tan(a)}}^{1}\int_{0}^{\frac{\tan(z(a))}{\tan(a)}}f_1(x,y)dydx\\&+\int_{Q^x}^{P^x}\int_{r_2}^{s_2}f_2(x,y)dydx+\int_{P^x}^{\frac{1}{\tan(a)}}\int_{r_2}^{r_1}f_2(x,y)dydx\\&+\int_{0}^{P^x}\int_{s_3}^{1}f_3(x,y)dydx+\int_{P^x}^{\frac{1}{\tan(a)}}\int_{r_1}^{1}f_3(x,y)dydx\\&+\int_{\frac{1}{\tan(a)}}^{1}\int_{\frac{\tan(z(a))}{\tan(a)}}^{1}f_4(x,y)dydx\Bigg)\end{aligned} \tag{40}$$

Case (IV) and Case (V)

$$D_{12}^{A}=\frac{1}{A_A}\left(\int_{0}^{Q^x}\int_{0}^{r_2}f_1(x,y)dydx+\int_{Q^x}^{Q'^x}\int_{0}^{s_1}f_1(x,y)dydx+\int_{0}^{Q^x}\int_{r_2}^{r_1}f_2(x,y)dydx+\int_{Q^x}^{P^x}\int_{s_2}^{r_1}f_2(x,y)dydx+\int_{0}^{P^x}\int_{r_1}^{s_3}f_3(x,y)dydx\right) \tag{41}$$

$$\begin{aligned}D_{12}^{B}=\frac{1}{A_B}\Bigg(&\int_{Q^x}^{\frac{1}{\tan(a)}}\int_{s_1}^{r_2}f_1(x,y)dydx+\int_{\frac{1}{\tan(a)}}^{Q'^x}\int_{s_1}^{\frac{\tan(z(a))}{\tan(a)}}f_1(x,y)dydx\\&+\int_{Q'^x}^{1}\int_{0}^{\frac{\tan(z(a))}{\tan(a)}}f_1(x,y)dydx+\int_{Q^x}^{P^x}\int_{r_2}^{s_2}f_2(x,y)dydx\\&+\int_{P^x}^{\frac{1}{\tan(a)}}\int_{r_2}^{r_1}f_2(x,y)dydx+\int_{0}^{P^x}\int_{s_3}^{1}f_3(x,y)dydx\\&+\int_{P^x}^{\frac{1}{\tan(a)}}\int_{r_1}^{1}f_3(x,y)dydx+\int_{\frac{1}{\tan(a)}}^{1}\int_{\frac{\tan(z(a))}{\tan(a)}}^{1}f_4(x,y)dydx\Bigg)\end{aligned} \tag{46}$$

Integrals to get D_{13} terms

$$\begin{aligned}D_{13}^{A}=\frac{1}{A_A}\Bigg(&\int_{0}^{Q_A^x}\int_{0}^{r_2}f_1(x,y)dydx+\int_{Q_A^x}^{Q_A'^x}\int_{0}^{s_{1A}}f_1(x,y)dydx\\&+\int_{0}^{Q_A^x}\int_{r_2}^{r_1}f_2(x,y)dydx+\int_{Q_A^x}^{P_A^x}\int_{s_{2A}}^{r_1}f_2(x,y)dydx\\&+\int_{0}^{P_A^x}\int_{r_1}^{s_{3A}}f_3(x,y)dydx\Bigg)\end{aligned} \tag{47}$$

$$\begin{aligned}D_{13}^{B}=\frac{1}{A_B}\Bigg(&\int_{Q_A^x}^{Q_A'^x}\int_{s_{1A}}^{r_2}f_1(x,y)dydx+\int_{Q_A'^x}^{Q_B^x}\int_{0}^{r_2}f_1(x,y)dydx\\&+\int_{Q_B^x}^{Q_B'^x}\int_{0}^{s_{1B}}f_1(x,y)dydx+\int_{Q_A^x}^{P_A^x}\int_{r_2}^{s_{2A}}f_2(x,y)dydx\\&+\int_{P_A^x}^{Q_B^x}\int_{r_2}^{r_1}f_2(x,y)dydx+\int_{Q_B^x}^{P_B^x}\int_{s_{2B}}^{r_1}f_2(x,y)dydx\\&+\int_{0}^{P_A^x}\int_{s_{3A}}^{s_{3B}}f_3(x,y)dydx+\int_{P_A^x}^{P_B^x}\int_{r_1}^{s_{3B}}f_3(x,y)dydx\Bigg)\end{aligned} \tag{48}$$

$$\begin{aligned}D_{13}^{C}=\frac{1}{A_C}\Bigg(&\int_{Q_B^x}^{Q_B'^x}\int_{s_{1B}}^{r_2}f_1(x,y)dydx+\int_{Q_B'^x}^{1}\int_{0}^{r_2}f_1(x,y)dydx\\&+\int_{Q_B^x}^{P_B^x}\int_{r_2}^{s_{2B}}f_2(x,y)dydx+\int_{P_B^x}^{1}\int_{r_2}^{r_1}f_2(x,y)dydx\\&+\int_{0}^{P_B^x}\int_{s_{3B}}^{1}f_3(x,y)dydx+\int_{P_B^x}^{1}\int_{r_1}^{1}f_3(x,y)dydx\Bigg)\end{aligned} \tag{49}$$

Integrals to get D_{22} terms

$$\begin{aligned}D_{22}^{A}=\frac{1}{A_A}\Bigg(&\int_{0}^{Q^x}\int_{0}^{r_4}f_1(x,y)dydx+\int_{Q^x}^{Q'^x}\int_{0}^{s_1}f_1(x,y)dydx\\&+\int_{0}^{Q^x}\int_{r_4}^{r_3}f_2(x,y)dydx+\int_{Q^x}^{P^x}\int_{s_2}^{r_3}f_2(x,y)dydx\\&+\int_{0}^{Q''^x}\int_{r_3}^{r_2}f_3(x,y)dydx+\int_{Q''^x}^{P^x}\int_{r_3}^{s_3}f_3(x,y)dydx\\&+\int_{0}^{Q''^x}\int_{r_2}^{r_1}f_4(x,y)dydx+\int_{Q''^x}^{P''^x}\int_{s_4}^{r_1}f_4(x,y)dydx\\&+\int_{0}^{P''^x}\int_{r_1}^{s_5}f_5(x,y)dydx\Bigg)\end{aligned} \tag{50}$$

$$\begin{aligned}D_{22}^{B}=\frac{1}{A_B}\Bigg(&\int_{Q^x}^{Q'^x}\int_{s_1}^{r_4}f_1(x,y)dydx+\int_{Q'^x}^{1}\int_{0}^{r_4}f_1(x,y)dydx\\&+\int_{Q^x}^{P^x}\int_{r_4}^{s_2}f_2(x,y)dydx+\int_{P^x}^{1}\int_{r_4}^{r_3}f_2(x,y)dydx\\&+\int_{Q''^x}^{P^x}\int_{s_3}^{r_2}f_3(x,y)dydx+\int_{P^x}^{1}\int_{r_3}^{r_2}f_3(x,y)dydx\\&+\int_{Q''^x}^{P''^x}\int_{r_2}^{s_4}f_4(x,y)dydx+\int_{P''^x}^{1}\int_{r_2}^{r_1}f_4(x,y)dydx\\&+\int_{0}^{P''^x}\int_{s_5}^{1}f_5(x,y)dydx+\int_{P''^x}^{1}\int_{r_1}^{1}f_5(x,y)dydx\Bigg)\end{aligned} \tag{51}$$

Integrals to get D_{23} terms

$$\begin{aligned}D_{23}^{A}=\frac{1}{A_A}\Bigg(&\int_{0}^{Q_A^x}\int_{0}^{r_4}f_1(x,y)dydx+\int_{Q_A^x}^{Q_A'^x}\int_{0}^{s_{1A}}f_1(x,y)dydx\\&+\int_{0}^{Q_A^x}\int_{r_4}^{r_3}f_2(x,y)dydx+\int_{Q_A^x}^{P_A^x}\int_{s_{2A}}^{r_3}f_2(x,y)dydx\\&+\int_{0}^{Q_A''^x}\int_{r_3}^{r_2}f_3(x,y)dydx+\int_{Q_A''^x}^{P_A^x}\int_{r_3}^{s_{3A}}f_3(x,y)dydx\\&+\int_{0}^{Q_A''^x}\int_{r_2}^{r_1}f_4(\mathrm{x},y)dydx+\int_{Q_A'^x}^{P_A''^x}\int_{s_{4A}}^{r_1}f_4(x,y)dydx\\&+\int_{0}^{P_A''^x}\int_{r_1}^{s_{5A}}f_5(x,y)dydx\Bigg)\end{aligned} \tag{52}$$

$$D_{23}^{B}=\frac{1}{A_B}\left(\int_{Q_A^x}^{Q_A'^x}\int_{s_{1A}}^{r_4}f_1(x,y)dydx+\int_{Q_A'^x}^{Q_B^x}\int_{0}^{r_4}f_1(x,y)dydx\right. \quad (53)$$
$$+\int_{Q_B^x}^{Q_B'^x}\int_{0}^{s_{1B}}f_1(x,y)dydx+\int_{Q_A^x}^{P_A^x}\int_{r_4}^{s_{2A}}f_2(x,y)dydx$$
$$+\int_{P_A^x}^{Q_B^x}\int_{r_4}^{r_3}f_2(x,y)dydx+\int_{Q_B^x}^{P_B^x}\int_{s_{2B}}^{r_3}f_2(x,y)dydx$$
$$+\int_{Q_A''^x}^{P_A^x}\int_{s_{3A}}^{r_2}f_3(x,y)dydx+\int_{P_A^x}^{Q_B''^x}\int_{r_3}^{r_2}f_3(x,y)dydx$$
$$+\int_{Q_B''^x}^{P_B^x}\int_{r_3}^{s_{3B}}f_3(x,y)dydx+\int_{Q_A''^x}^{P_A''^x}\int_{r_2}^{s_{4A}}f_4(x,y)dydx$$
$$+\int_{P_A''^x}^{Q_B''^x}\int_{r_2}^{r_1}f_4(x,y)\mathrm{d}ydx+\int_{Q_B''^x}^{P_B''^x}\int_{s_{4B}}^{r_1}f_4(x,y)dydx$$
$$\left.+\int_{0}^{P_A''^x}\int_{s_{5A}}^{s_{5B}}f_5(x,y)dydx+\int_{P_A''^x}^{P_B''^x}\int_{r_1}^{s_{5B}}f_5(x,y)dydx\right)$$

$$D_{23}^{C}=\frac{1}{A_C}\left(\int_{Q_B^x}^{Q_B'^x}\int_{s_{1B}}^{r_4}f_1(x,y)dydx+\int_{Q_B'^x}^{1}\int_{0}^{r_4}f_1(x,y)dydx\right. \quad (54)$$
$$+\int_{Q_B^x}^{P_B^x}\int_{r_4}^{s_{2B}}f_2(x,y)dydx+\int_{P_B^x}^{1}\int_{r_4}^{r_3}f_2(x,y)dydx$$
$$+\int_{Q_B''^x}^{P_B^x}\int_{s_{3B}}^{r_2}f_3(x,y)dydx+\int_{P_B^x}^{1}\int_{r_3}^{r_2}f_3(x,y)dydx$$
$$+\int_{Q_B''^x}^{P_B''^x}\int_{r_2}^{s_{4B}}f_4(x,y)dydx+\int_{P_B''^x}^{1}\int_{r_2}^{r_1}f_4(x,y)dydx$$
$$\left.+\int_{0}^{P_B''^x}\int_{s_{5B}}^{1}f_5(x,y)dydx+\int_{P_B''^x}^{1}\int_{r_1}^{1}f_5(x,y)dydx\right)$$

References

1. Horta M, Coelho F, Relvas S (2016) Layout design modelling for a real world just-in-time warehouse. Comput Ind Eng 101:1–9
2. Zhang G, Nishi T, Turner SDO, Oga K, Li X (2017) An integrated strategy for a production planning and warehouse layout problem: modeling and solution approaches. Omega 68:85–94
3. Boysen N, de Koster R, Weidinger F (2018) Warehousing in the e-commerce era: a survey. Eur J Oper Res
4. Gu J, Goetschalckx M, McGinnis L (2007) Research on warehouse operation: a comprehensive review. Eur J Oper Res 177(1):1–21
5. Rouwenhorst B, Reuter B, Stockrahm V, van Houtum G, Mantel R, Zijm W (2000) Warehouse design and control: framework and literature review. Eur J Oper Res 122:515–533
6. Baker P, Canessa M (2009) Warehouse design: a structured approach. Eur J Oper Res 193:425–436
7. Gu J, Goetschalckx M, McGinnis L (2010) Research on warehouse design and performance evaluation: a comprehensive review. Eur J Oper Res 203(3):539–549
8. Cormier G, Gunn EA (1992) A review of warehouse models. Eur J Oper Res 58:3–13
9. Accorsi R, Bortolini M, Gamberi M, Manzini R, Pilati F (2017) Multi-objective warehouse building design to optimize the cycle time, total cost, and carbon footprint. Int J Adv Manuf Technol 92(1–4):839–854
10. Staudt FH, Alpan G, Di Mascolo M, Taboada Rodriguez CM (2015) Warehouse performance assessment: a literature review. Int J Prod Res 53(18):5524–5544
11. Dotoli M, Epicoco N, Falagario M, Costantino N, Turchiano B (2015) An integrated approach for warehouse analysis and optimization: a case study. Comput Ind 70:56–69
12. Gue KR, Meller RD (2009) Aisle configurations for unit-load warehouses. IIE Trans 41(3):171–182
13. De Koster R, Le-Duc T, Roodbergen KJ (2007) Design and control of warehouse order picking: a literature review. Eur J Oper Res 182:481–501
14. Bartholdi JJ, Hackman ST (2017) Warehouse and distribution science, version 0.98. https://www.warehouse-science.com/book/editions/wh-sci-0.98.pdf. Accessed 5 February 2018
15. Roodbergen KJ, De Koster R (2001) Routing order pickers in a warehouse with a middle aisle. Eur J Oper Res 133:32–43
16. Accorsi R, Manzini R, Maranesi F (2014) A decision-support system for the design and management of warehousing systems. Comput Ind 65:175–186
17. Öztürkoglu O, Gue KR, Meller RD (2012) Optimal unit-load warehouse designs for single-command operations. IIE Trans 44:459–475
18. Le-Duc T, De Koster R (2005) Travel distance estimation and storage zone optimization in a 2-block class-based storage strategy warehouse. Int J Prod Res 43(17):3561–3581
19. Hausman WH, Schwarz LB, Graves SC (1976) Optimal storage assignment in automatic warehousing systems. Manag Sci 22(6):629–638
20. Bortolini M, Accorsi R, Gamberi M, Manzini R, Regattieri A (2015) Optimal design of AS/RS storage systems with three-class-based assignment strategy under single and dual command operations. Int J Adv Manuf Technol 79(9–12):1747–1759
21. Zaerpour N, Yu Y, de Koster RBM (2017) Optimal two-class-based storage in a live-cube compact storage system. IISE Trans 49(7):653–668
22. Bortolini M, Faccio M, Gamberi M, Manzini R (2015) Diagonal cross-aisle in unit-load warehouses to increase handling performance. Int J Prod Econ 170:838–849
23. Gabbard M, Reinholdt E (1975) Warehouse cost analysis. West Electr Eng 19:52–60
24. Rai D, Sodegar B, Fieldson R, Hu X (2011) Assessment of CO_2 emissions reduction in a distribution warehouse. Energy 36:2271–2277
25. Chew EP, Tang LC (1999) Cycle time analysis for general item location assignment in a rectangular warehouse. Eur J Oper Res 112:582–597
26. Wang G, Feng G, Kang Z, Wang H (2017) Research on the heat load of food freezing in refrigerated warehouse. Procedia Eng 205:1843–1849
27. Bortolini M, Faccio M, Ferrari E, Gamberi M, Pilati F (2016) Fresh food sustainable distribution: cost, delivery time and carbon footprint three-objective optimization. J Food Eng 174:56–67
28. Ding B (2018) Pharma Industry 4.0: literature review and research opportunities in sustainable pharmaceutical supply chains. Process Saf Environ Prot 119:115–130
29. Liu X, Li J, Li X (2017) Study of dynamic risk management system for flammable and explosive dangerous chemicals storage area. J Loss Prev Process Ind 49:983–988
30. Khakzad N, Van Gelder P (2017) Fragility assessment of chemical storage tanks subject to floods. Process Saf Environ Prot 111:75–84
31. Bassan Y, Roll Y, Rosenblatt MJ (1980) Internal layout design of a warehouse. IIE Trans 12(4):317–322

32. White J (1972) Optimum design of warehouses having radial aisles. AIIE Trans 4(4):333–336
33. Arlinghaus SL, Nystuen JD (1991) Street geometry and flows. Geogr Rev 81(2):206–214
34. Clark KA, Meller RD (2013) Incorporating vertical travel into non-traditional cross-aisles for unit-load warehouse designs. IIE Trans 45(12):1322–1331
35. Cardona LF, Soto DF, Rivera L, Martínez HJ (2015) Detailed design of fishbone warehouse layouts with vertical travel. Int J Prod Econ 170:825–837
36. Çelk M, Süral H (2014) Order picking under random and turnover-based storage policies in fishbone aisle warehouses. IIE Trans 46(3):283–300
37. Pohl LM, Meller RD, Gue KR (2009) An analysis of dual-command operations in common warehouse designs. Transport Res E-Log 45(3):367–379
38. Pohl LM, Meller RD, Gue KR (2009) Optimizing fishbone aisles for dual-command operations in a warehouse. Nav Res Logist 56(5):389–403
39. Gue KR, Ivanovic G, Meller RD (2012) A unit-load warehouse with multiple pickup and deposit points and non-traditional aisles. Transp Res E 48(4):795–806
40. Thomas LM, Meller RD (2014) Analytical models for warehouse configuration. IIE Trans 46(9):928–947
41. Pferschy U, Schauer J (2018) Order batching and routing in a non-standard warehouse. Electron Notes Discrete Math 69:125–132
42. Heskett J (1963) Cube-per-order index: a key to warehouse stock location. Transp Distrib Manag 3:27–31
43. Kallina C, Lynn J (1976) Application of the cube-per-order index rule for stock location in a distribution warehouse. Interfaces 7:37–46
44. Manzini R, Gamberi M, Persona A, Regattieri A (2007) Design of a class based storage picker to product order picking system. Int J Adv Manuf Technol 32(7–8):811–821
45. Larson TN, March H, Kusiak A (1997) Heuristic approach to warehouse layout with class-based storage. IIE Trans 29(4):337–348
46. Kovács A (2011) Optimizing the storage assignment in a warehouse served by milkrun logistics. Int J Prod Econ 133(1):312–318
47. Ene S, Öztürk N (2012) Storage location assignment and order picking optimization in the automotive industry. Int J Adv Manuf Technol 60(5–8):787–797
48. Rao SS, Adil GK (2013) Class-based storage with exact S-shaped traversal routing in low-level picker-to-part systems. Int J Prod Res 51(16):4979–4996
49. Yu Y, De Koster R (2013) On the suboptimality of full turnover-based storage. Int J Prod Res 51(6):1635–1647
50. Ekren BY, Sari Z, Lerher T (2015) Warehouse design under class-based storage policy of shuttle-based storage and retrieval system. IFAC Pap Online 48(3):1152–1154
51. Flores B, Whybark C (1986) Multiple criteria ABC analysis. Int J Oper Prod Manag 6:38–46
52. Lolli F, Ishizaka A, Gamberini R, Rimini B (2017) A multicriteria framework for inventory classification and control with application to intermitted demand. J Multi-Criteria Decis Anal 24:275–285
53. Lolli F, Ishizaka A, Gamberini R (2014) New AHP-based approaches for multi-criteria inventory classification. Int J Prod Econ 156:62–74
54. Ishizaka A, Lolli F, Balugani E, Cavallieri R, Gamberini R (2018) DEASort: assigning items with data envelopment analysis in ABC classes. Int J Prod Econ 199:7–15
55. Soylu B, Akyol B (2014) Multi-criteria inventory classification with reference items. Comput Ind Eng 69:12–20
56. Douissa MR, Jabeur K (2016) A new model for multi-criteria ABC inventory classification: PROAFTN method. Procedia Comput Sci 96:550–559
57. Torabi SA, Hatefi SM, Salek Pay B (2012) ABC inventory classification in the presence of both quantitative and qualitative criteria. Comput Ind Eng 63:530–537
58. Bonnans JF, Gilbert JC, Lemaréchal C, Sagastizábal CA (2006) Numerical optimization: theoretical and practical aspects. Universitext (Second revised ed. of translation of 1997 French ed.) Springer-Verlag, Berlin